# Thrombogenic potential of transcatheter aortic valve implantation with trivial paravalvular leakage

Lawrence N. Scotten[1], Rolland Siegel[2]

[1]ViVitro Systems Inc. (VSI), Victoria, B.C., Canada; [2]90 Garibaldi Street, Lake Oswego, OR, USA
*Correspondence to:* Lawrence N. Scotten. Dipl. T., Director, ViVitro Systems Inc., (VSI), 6-1560 Church Avenue, Victoria, B.C., V8P 2H1, Canada. Email: larryscotten2@hotmail.com.

**Background:** Significant paravalvular leakage after transcatheter aortic valve implantation (TAVI) correlates with increased morbidity and mortality, but adverse consequences of trivial paravalvular leakage have stimulated few investigations. Using a unique method distinctly different from other diagnostic approaches, we previously reported elevated backflow velocities of short duration (transients) in mechanical valve closure. In this study, similar transients were found in a transcatheter valve paravalvular leakage avatar.

**Methods:** Paravalvular leakage rate (zero to 58 mL/second) and aortic valve incompetence (volumetric back flow/forward flow; zero to 32%) were made adjustable using a mock transcatheter aortic valve device and tested in quasi-steady and pulsatile flow test systems. Projected dynamic valve area (PDVA) from the back illuminated mock transcatheter aortic valve device was measured and regional backflow velocities were derived by dividing volumetric flow rate by the PDVA over the open and closing valve phase and the total closed valve area derived from backflow leakage.

**Results:** Aortic incompetence from 1-32% generated negative backflow transients from 8 to 267 meters/second, a range not dissimilar to that measured in mechanical valves with zero paravalvular leakage. Optimal paravalvular leakage was identified; not too small generating high backflow transients, not too large considering volume overload and cardiac energy loss caused by defective valve behavior and fluid motion.

**Conclusions:** Thrombogenic potential of transcatheter aortic valves with trivial aortic incompetence and high magnitude regional backflow velocity transients was comparable to mechanical valves. This may have relevance to stroke rate, asymptomatic microembolic episodes and indications for anticoagulation therapy after transcatheter valve insertion.

**Keywords:** Transcatheter aortic valve implantation (TAVI); paravalvular; leakage; transients; incompetence

## Introduction

There has been increasing use of transcatheter aortic valve implantation (TAVI) since clinical introduction in 2002 by Cribier and associates (1). Subsequently, TAVI has emerged as a therapeutic option for high-risk patients with severe aortic disease who are not candidates for surgical aortic valve replacement (SAVR) (2). More than 80,000 patients have experienced this therapy and the number is increasing (3). One reported complication with TAVI procedures is elevated early and late stroke rate compared to SAVR (4,5). Although significant paravalvular leak (PVL) after TAVI procedures

increases morbidity and mortality, adverse consequences of trivial PVL, with a reported incidence of 40-70%, have stimulated few investigations (6). Unlike SAVR valves that incorporate a compliant external sewing ring to ensure a haemostatic seal, TAVI relies on in-situ expansion of a generic metallic mesh frame partially covered with porous fabric to achieve deployment and a full haemostatic seal requires successful tissue ingrowth. Annulus calcification and other factors pose a risk of residual PVL. A further limitation may be a PVL initiated thromboembolic component similar to that which we reported in mechanical heart valves (MHVs)

Page 2 of 10

Scotten and Siegel. Thrombogenic potential of TAVI with trivial PVL

in a previous study (7).

## Materials and methods

*Figure 1* illustrates a TAVI device (Sapien XT) and an Edwards-Perimount Model 2800 pericardial valve (Edwards Lifesciences Inc., Irvine, California, USA) of tissue annulus diameter, TAD 25 mm assembled in an adjustable PVL fixture as a mock-TAVI (mTAVI). The mechanism depicted in the lower panel of *Figure 1* allowed for leakage testing with varied pre-set PVLs. Pulsatile flow testing of the mTAVI was then conducted using a modified pulse duplicator with Leonardo$^{VSI}$ Technology installed (ViVitro Systems Inc., Victoria, Canada).

Recognizing that the complex motion of prosthetic valves is too fast to see, and too important to ignore, we constructed a unique prototype electro-optical attachment (Leonardo$^{VSI}$) and incorporated it into our modified pulse duplicator as a practical way to pre-calibrate, record, and perform quantitative analysis of valve motion. Furthermore, this new technique provides a spatial average of flow velocities in immediate proximity to valves. Based on our prior work, we suggest that elevated valve closure transients are a primary cause of blood cell damage and subsequent initiation of thrombogenic response. Their assessment offers the potential to quantitatively screen valves for relative thrombogenic potential (7).

The mTAVI was initially tested in a closed state within a leakage tester to preset PVL under quasi-steady transvalvular back pressure conditions (range 80-120 mmHg; mean 100 mmHg). The mTAVI was then mounted in the modified pulse duplicator to test under pulsatile flow conditions: pulse rate 70 beats/min; aortic pressures ≈120/80 mmHg; net forward flow rate (cardiac output) of 5 L/min. The mitral non-test valve was a Mitroflow 29 mm pericardial valve (Sorin S.p.A., Milan, Italy). To maintain stable optical and viscous properties, the test fluid was saline with viscosity 1 mPa·s and density 1.0 g/mL. Other authors, using an SJM valve (St. Jude Medical, St. Paul, Minnesota, USA), had shown fluid viscosities ranging from 1.1 to 3.1 mPa·s to have a negligible effect on the valve-closing PDVA, but reduced the volumetric backflow rate by ≈14% (8). Further experimental and methodological details can be found in supplementary (S) materials and methods .

## Results

Typical waveform dynamics are shown in *Figure 2A* and *2B* for the mTAVI device tested under varied aortic incompetence (AI). Most noteworthy are significant
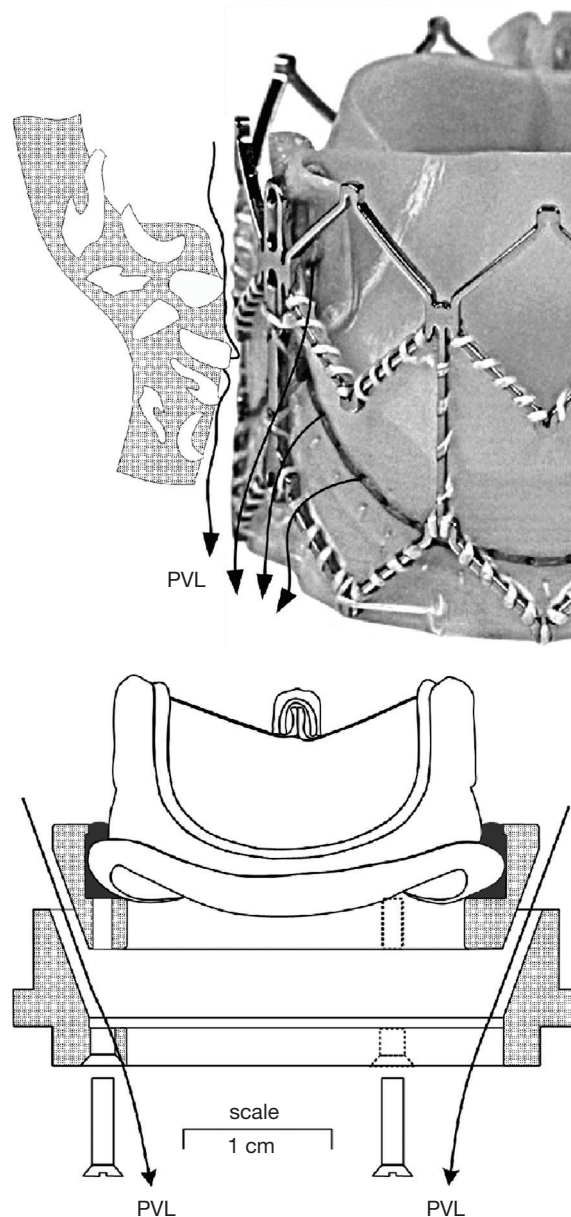


**Figure 1** Depiction of implanted Edwards Sapien XT TAVI with paravalvular leakage (PVL) through calcified irregular and tortuous pathways, indicated by arrows, resulting from tissue calcification (upper panel). The mock-TAVI (mTAVI) device is mounted within an adjustable PVL mechanism (lower panel). Differences in leaflet dynamics and geometry between the valves are assumed minor. The mTAVI device fabric was sealed with silicone rubber to reduce intravalvular leakage to ≈ –1.35 mL/s.

differences in backflow transients (RBV$_{-max}$) near valve closure. We observed that greater PVL and AI was

consistently associated with a relative absence of these high magnitude backflow transients. Backflow transients are summarized in *Figure 3* showing $RBV_{-max}$ versus AI and indicates an optimal range having low backflow transients, low potential for activation of coagulation factors, and below thresholds considered to have significant volume overload and energy loss. Additional waveforms are found in the Supplementary (S).

## Discussion

### Thrombogenic impact of intra and perivalvular leakage

Forward flow detail has preoccupied fluid dynamics heart valve studies, thus overlooking high magnitude transients generated during valve closure. Recent innovative *in vitro* inferential technique (7) identified a major thrombogenic component related to supraphysiologic RBV transients in MHV closure but absent in tissue valve closure (7). Data from that study suggest that closure dynamics and trivial leakage areas produce a contribution to valve thrombogenic potential. Recently, a CFD study stated that "…vortices generated in the valve closure and regurgitant period encompass important mechanism which was overlooked in the past" (9). While there is consensus that elevated velocity gradients in flowing blood (shear rate) damages blood cells, opinions vary greatly as to the range of shear rate harmful to cells (10). Nonetheless, greater shear rate levels are inferred by an $RBV_{-max}$ increase.

Pathological fluid forces may elicit a coagulation response for all valve types. The greatest disruption to normal physiologic flow occurs near valve closure when transient flow velocity (±m/s), accelerating (+m/s$^2$), decelerating (–m/s$^2$), and jerk defined as rate of acceleration (±m/s$^3$) fluid flows predominate. Such flows have potential for elevated shear rates and stagnant flows. Once fluid shear has initiated multiple biochemical and functional reactions, micro-thrombi aggregates form that may attach locally or embolize. For MHVs, cyclic closure flow transients appear to be related to a prothrombotic state requiring chronic anti-coagulation. Current model tissue bioprostheses appear not to generate a pro-thrombotic closing phase but TAVI prostheses with trivial PVL may generate pathologic flow transients similar to those observed in MHVs. Although several complex mechanisms are responsible for thrombogenesis (11), contributions causing hemolysis appear negligible a propos valve function and except for isolated cases, acceleration of red cell degeneration after

MHV implantation is inconsequential (12). Thrombogenic response to valves is primarily initiated by flow induced shear rate damage to formed blood elements including red and white cells and platelets. In current MHVs, extreme transient shear rate conditions have been found near valve closure caused by backflow through residual gap areas (13,14) and are often present in immediate proximity to TAVI devices. We have noted a simple hydraulic relationship; for a given volumetric backflow rate near valve closure, the smaller the total residual leakage area, the greater the magnitude of the backflow transients. Thus, our experiments substantiate that under different PVL conditions similar regurgitant volume rates occur during moments near valve closure and that smaller leakage areas intrinsically lead to higher $RBV_{-max}$ transients (see *Figure 2A* and *2B*). This is strikingly illustrated in *Figure 3*, where the exponential relationship between trivial AI and $RBV_{-max}$ is denoted by the vertical dashed lines within the >0 to 5% AI range and implies elevated thrombogenic potential. The critical $RBV_{-max}$ threshold for activation of clotting mechanisms is unknown, but velocities exceeding those observed in standard stented tissue bioprostheses reported by us previously (7) are of concern. Blood borne tissue factors, considered a key component in biochemical initiation of the coagulation cascade (15,16), can shed into the blood stream from shear rate-damaged blood components, along with other pro-coagulant agents (17). In addition, flows that are close to sharp edges, steps, or narrow gaps between valve components can generate low-shear rate regions or 'hot spots' that trap and aggregate activated platelets (13). Calcified paravalvular pathways may include such sharp edges, steps or narrow irregular gaps. The magnitude of platelet activation and aggregation is likely to correlate with the flow velocity, acceleration, and jerk indicative of pathologic fluid force intensity during the closing phase (18).

### Clinical implications

Calcification of TAVI implant sites is frequently reported (19). Procedure associated physical manipulations are suspect in migration of calcific debris and an incidence of early (acute) stroke (20,21). The etiology of late (non-acute) stroke after TAVI is less apparent and perhaps more related to pathologic flow conditions within or adjacent to the implant. Using typical TTE/TEE techniques, cases in which the AI grade is "none", the presence/absence of backflow velocities of high transient amplitude and short duration (<10 ms) cannot be resolved in immediate proximity to valves, owing to
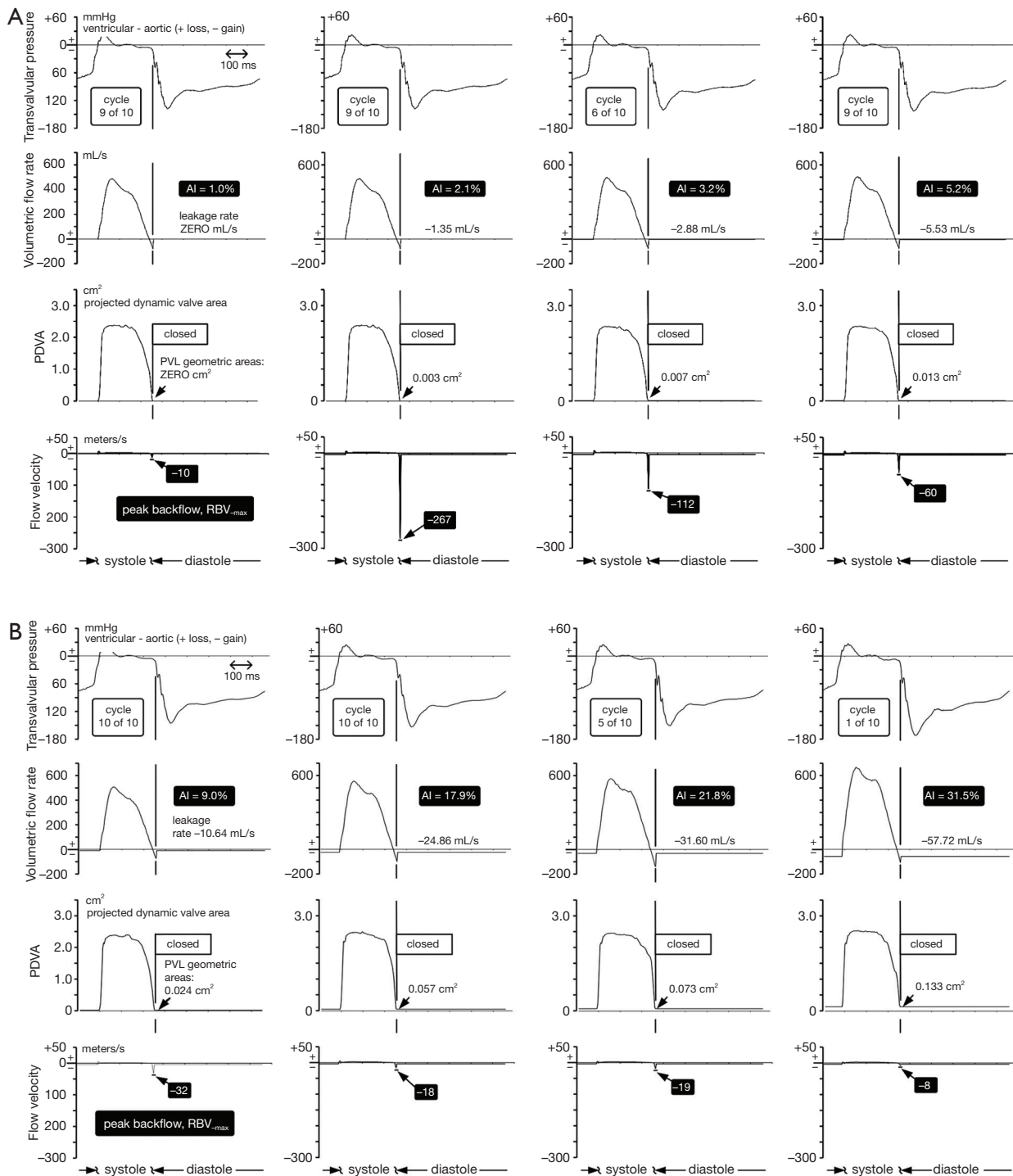
**Page 4 of 10**

**Scotten and Siegel. Thrombogenic potential of TAVI with trivial PVL**



**Figure 2** (A) Hydrodynamic and valve motion (PDVA) waveforms for mock-TAVI (mTAVI) device using Edwards-Perimount valve size 25 mm. Aortic valve incompetence (AI) range is trivial (1.0-5.2%). Cycles shown are those that gave the greatest backflow transients of the ten consecutive cycles acquired. Heart Rate 70/min; cardiac output 5 liters/minute; test fluid saline; mean systolic aortic pressure ≈100 mmHg; (B) AI range is mild (9.0-31.5%). See *Figure 2A* caption for other test conditions.
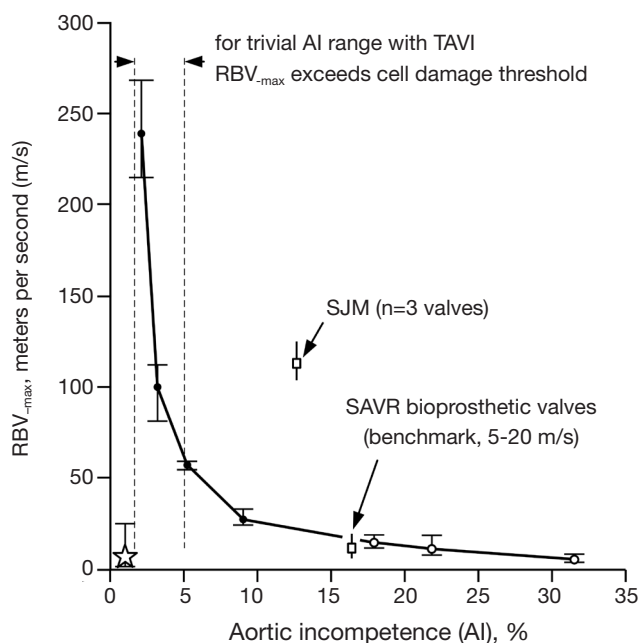
**Figure 3** The mock-TAVI (mTAVI) device under various paravalvular conditions with aortic valve incompetence (AI) =1-32%. The ideal TAVI paravalvular condition (Star data point) is AI near ZERO. This negates large transients of regional backflow velocity (RBV$_{-max}$) where least thrombogenic potential is inferred. Black data points include trivial AI where intense transients generated by the closing valve infer high thrombogenic potential. White data points (AI>15%) have lower RBV$_{-max}$ flow transients, however, transvalvular energy loss will increase during the closed valve interval with AI increase. The mean RBV$_{-max}$ and range of variation for each experiment are shown (vertical bars, n=10 consecutive cycles). Suggested thrombogenic benchmark based on testing several bioprostheses with no paravalvular leakage (PVL) is shown for surgical aortic valve replacement (SAVR) reference. St Jude Medical (SJM) size 25 mm valve results is also shown for SAVR reference for a mechanical heart valve (MHV) with PVL = zero.

multiple technical shortcomings e.g., sensitivity, precision, spaciotemporal resolution, and imaging planes. These limitations may be obscuring important prothrombotic data. Therefore, it may be productive to examine non-acute stroke rates as well as the incidence and effects of repeated micro-embolic episodes referred to as "asymptomatic" (22) after TAVI procedures to establish a direct relationship between this retrograde flow phenomenon and adverse clinical events. Study of cerebral micro-emboli and cerebrovascular symptoms by transcranial Doppler and measurement of platelet derived micro-particles described by Skjelland and

associates (23) after TAVI may also yield important insight regarding causal relationships between pathologic retrograde flow transients and stroke.

Although the medical literature is replete with articles on echocardiographic assessment of valvular regurgitation (24,25), none have reported transient backflows approaching the RBV$_{-max}$ observed in this study. In the clinical setting, continuous wave (CW) Doppler echocardiography is used to measure high-velocity flows in part because the Nyquist limit is not applicable with CW reception of the Doppler signal (26). Although the increased imaging resolution of TEE is advantageous, this technique can only accurately measure high velocity flows up to 9 m/s along the beam axis parallel to flow (27). Extreme transients in immediate proximity to the valve with peak backflow velocities of up to 300 m/s and duration of <10 ms, appear well beyond detection by current TEE equipment. Simply stated, currently available TEE equipment cannot "see" velocities indicated by our study data. Measurement of high transient backflows or their consequences in patients remains challenging, and we are unaware of data directly linking RBVs to stroke. In a separate internal study, a range of valve thrombogenic potential based on measurement of RBV$_{-max}$ transients on 12 aortic pericardial and porcine bioprostheses, was ≈5 to 20 m/s. In *Figure 3*, this low thrombogenic benchmark is superimposed on the mTAVI device results where the upper range limit first coincides at AI of ≈16%. The benchmark may represent an optimal or "Goldilocks zone"—not too small to cause high flow transients and activation of coagulation factors and not too large to cause significant volume overload and energy loss. These parameters may be important for future valve development and modification.

### Caveats

Although the function of the mTAVI device did not precisely replicate the *in vitro* behavior of a Sapien XT valve, the resolution capabilities of our methodology provided observational and quantitative information about TAVI function and PVL not previously reported. While not a site specific quantity, we submit that RBV$_{-max}$ is a useful surrogate for flow induced blood cell damage potential.

The paravalvular leakage pathways in *Figure 1*, (lower panel), represent uniform flow pathways, whereas more realistic retrograde flow pathways depicted in *Figure 1* (top panel) between implant exterior and anatomic site are likely to be tortuous and irregular. Whilst the adjustable mechanism we devised for changing PVL was less than

Page 6 of 10

Scotten and Siegel. Thrombogenic potential of TAVI with trivial PVL

ideal for mimicking complex PVL pathways, it did provide a practical way to obtain and specify geometric PVL areas, prior to pulse duplicator testing, via the leakage tester.

In conclusion, recent studies relating fluid shear rate to valve pro-thrombotic potential have identified crucial differences in bileaflet mechanical and tissue valve-closing response (7,28,29). This study is an extension of that work and uses improved technology to measure mTAVI device function along with the influence of preset PVLs. Our results infer shear rate damage to formed blood elements and resultant chronic thrombogenic response that constitute a fluid mechanical foundation to explain observed thrombogenic rates unique to individual prosthetic valve types and designs now broadened to include observations of TAVI related thromboembolic events. Our technology enabled regional flow velocity to be resolved and focused attention on overt flow transients previously overlooked and hidden due to brevity, small paravalvular spaces, and limited instrumentation capability. We hypothesize that elevated transients during the closing phase of the cardiac cycle may represent a primary factor in TAVI thrombogenesis particularly when trivial PVL is present and/or with greater AI within calcified and tortuous backflow pathways. Tissue valve leaflet closure, assisted by flow deceleration, reduces transvalvular pressures and backflow transients, leading to the lower thrombogenic potential generally associated with these valves compared to MHVs. However, when PVL is present after TAVI procedures, pathologic backflow velocity transients are possible. While this relationship is not fully understood or confirmed, we note that Latib and associates (30) have recommended chronic anticoagulation for patients undergoing TAVI procedures as with MHV recipients. Finally, Azadani and associates state "Paravalvular leak is expected to remain the major issue to be addressed in the next generation of TAVs, if TAV indications are expanded to younger and healthier patients" (31). Efforts to address this issue are stimulating diverse approaches including those described by Walther and coworkers wherein a modified TAVI device (Sapien + Cloth) was evaluated within an *in vitro* system simulating a valve-in-valve procedure with a standard Edwards Perimount bioprosthesis (32) and by Astarci and coworkers who suggest transcatheter resection of native valve leaflets to improve TAVI sizing accuracy for reduction of morbid events (33). While efforts to mitigate TAVI paravalvular leak are inevitable and justifiable, we draw attention to the unintended consequence of PVL reduction leading to "trivial" leak status with high $RBV_{-max}$ and increased thrombogenic potential.

## References

1. Cribier A, Eltchaninoff H, Bash A, et al. Percutaneous transcatheter implantation of an aortic valve prosthesis for calcific aortic stenosis: first human case description. Circulation 2002;106:3006-8.

2. Lawrie GM. Role of transcatheter aortic valve implantation (TAVI) versus conventional aortic valve replacement in the treatment of aortic valve disease. Methodist Debakey Cardiovasc J 2012;8:4-8.

3. Cribier A. Perspective on transcatheter aortic valve implantation: past, present, and future. Chin Med J (Engl) 2013;126:1008-12.

4. Sponga S, Perron J, Dagenais F, et al. Impact of residual regurgitation after aortic valve replacement. Eur J Cardiothorac Surg 2012;42:486-92.

5. Gripari P, Ewe SH, Fusini L, et al. Intraoperative 2D and 3D transoesophageal echocardiographic predictors of aortic regurgitation after transcatheter aortic valve implantation. Heart 2012;98:1229-36.

6. Vasa-Nicotera M, Sinning JM, Chin D, et al. Impact of paravalvular leakage on outcome in patients after transcatheter aortic valve implantation. JACC Cardiovasc Interv 2012;5:858-65.

7. Scotten LN, Siegel R. Importance of shear in prosthetic valve closure dynamics. J Heart Valve Dis 2011;20:664-72.

8. van Steenhoven AA, van Duppen TJ, Cauwenberg JW, et al. In vitro closing behaviour of Björk-Shiley, St Jude and Hancock heart valve prostheses in relation to the in vivo recorded aortic valve closure. J Biomech 1982;15:841-8.

9. Hsu UK, Lu PJ. Dynamic simulation and hemolysis evaluation of the regurgitant flow over a tilting-disc mechanical heart valve in pulsatile flow. World Journal of Mechanics 2013;3:160-8.

10. Brindley D, Moorthy K, Lee JH, et al. Bioprocess forces and their impact on cell behavior: implications for bone regeneration therapy. J Tissue Eng 2011;2011:620247.

11. Nesbitt WS, Westein E, Tovar-Lopez FJ, et al. A shear gradient-dependent platelet aggregation mechanism drives thrombus formation. Nat Med 2009;15:665-73.

12. Taggart DP, Spyt TJ, Wheatley DJ, et al. Severe haemolysis with the St. Jude Medical prosthesis. Eur J Cardiothorac Surg 1988;2:137-42.

13. Bluestein D, Chandran KB, Manning KB. Towards non-thrombogenic performance of blood recirculating devices. Ann Biomed Eng 2010;38:1236-56.

14. Rambod E, Beizai M, Sahn DJ, et al. Role of vortices in growth of microbubbles at mitral mechanical heart valve closure. Ann Biomed Eng 2007;35:1131-45.

15. Breitenstein A, Tanner FC, Lüscher TF. Tissue factor and cardiovascular disease: quo vadis? Circ J 2010;74:3-12.

16. Rodriguez RA, Ruel M, Labrosse M, et al. Transcranial Doppler and acoustic pressure fluctuations for the assessment of cavitation and thromboembolism in patients with mechanical heart valves. Interact Cardiovasc Thorac Surg 2008;7:179-83.

17. Goldsmith IR, Blann AD, Patel RL, et al. Effect of aortic valve replacement on plasma soluble P-selectin, von Willebrand factor, and fibrinogen. Am J Cardiol 2001;87:107-10, A9.

18. Prohaska W, Zittermann A, Lüth JU, et al. Prevalent platelet dysfunction in patients with aortic valve disease. J Heart Valve Dis 2008;17:542-7.

19. Haensig M, Rastan AJ. Aortic valve calcium load before TAVI: Is it important? Ann Cardiothorac Surg 2012;1:160-4.

20. Rodés-Cabau J, Dauerman HL, Cohen MG, et al. Antithrombotic treatment in transcatheter aortic valve implantation: insights for cerebrovascular and bleeding events. J Am Coll Cardiol 2013;62:2349-59.

21. Lynch DR Jr, Dantzler D, Robbins M, et al. Considerations in antithrombotic therapy among patients undergoing transcatheter aortic valve implantation. J Thromb Thrombolysis 2013;35:476-82.

22. Gress DR. The problem with asymptomatic cerebral embolic complications in vascular procedures: what if they are not asymptomatic? J Am Coll Cardiol 2012;60:1614-6.

23. Skjelland M, Michelsen A, Brosstad F, et al. Solid cerebral microemboli and cerebrovascular symptoms in patients with prosthetic heart valves. Stroke 2008;39:1159-64.

24. Pibarot P, Dumesnil JG. Doppler echocardiographic evaluation of prosthetic valve function. Heart 2012;98:69-78.

25. Zamorano JL, Badano LP, Bruce C, et al. EAE/ASE recommendations for the use of echocardiography in new transcatheter interventions for valvular heart disease. Eur Heart J 2011;32:2189-214.

26. Side CD, Gosling RG. Non-surgical assessment of cardiac function. Nature 1971;232:335-6.

27. Prabhu M, Raju D, Pauli H. Transesophageal echocardiography: instrumentation and system controls. Ann Card Anaesth 2012;15:144-55.

28. Borazjani I, Ge L, Sotiropoulos F. High-resolution fluid-structure interaction simulations of flow through a bi-leaflet mechanical heart valve in an anatomic aorta. Ann Biomed Eng 2010;38:326-44.

29. Simon HA, Ge L, Borazjani I, et al. Simulation of the three-dimensional hinge flow fields of a bileaflet mechanical heart valve under aortic conditions. Ann Biomed Eng 2010;38:841-53.

30. Latib A, Messika-Zeitoun D, Maisano F, et al. Reversible Edwards Sapien XT dysfunction due to prosthesis thrombosis presenting as early structural deterioration. J Am Coll Cardiol 2013;61:787-9.

31. Azadani AN, Jaussaud N, Matthews PB, et al. Energy loss due to paravalvular leak with transcatheter aortic valve implantation. Ann Thorac Surg 2009;88:1857-63.

32. Walther T, Dehdashtian MM, Khanna R, et al. Trans-catheter valve-in-valve implantation: in vitro hydrodynamic performance of the SAPIEN+cloth trans-catheter heart valve in the Carpentier-Edwards Perimount valves. Eur J Cardiothorac Surg 2011;40:1120-6.

33. Astarci P, Etienne PY, Raucent B, et al. Transcatheter resection of the native aortic valve prior to endovalve implantation - A rational approach to reduce TAVI-induced complications. Ann Cardiothorac Surg 2012;1:224-30.

## Supplementary (S)

## Methods and materials

### Adjustable and preset mTAVI paravalvular leakage mechanism

The apparatus in *Figure 1* (lower panel) consisted of two machined plastic parts (Delrin™) with 70° tapers. Plastic shims 6 each of length: 7.5 mm × width: 6 mm × various thicknesses: (0.07 to 0.29 mm) were spaced equally and clamped between the tapers with bolts. Thus, shim thickness established the total geometric area available for PVL flow between the two parts. Very minor changes in shim thickness significantly affected leakage rates and underscored the extremely small tolerances involved in creating "trivial" aggregated leakage areas associated with high velocity backflow transients. For example, increasing or decreasing shim thickness by 0.07 mm changes aggregate PVL area by 0.004 mm$^2$. This finding calls attention to the role of calcification in creating multiple micro-pathways involving complex small scale flows with potential for high backflow velocities and shear rates. The Edwards Perimount is characterized by a small volume of leakage through the frame. To mitigate the leakage differences between a clinical Sapien XT and Perimount bioprosthesis, the mTAVI device fabric and compliant sewing ring were sealed with RTV silicone rubber Dow Corning, (#732) to minimize intravalvular leakage to ≈–1.35 mL/s under a mean transvalvular pressure of 100 mmHg. For comparison, it has been reported that an actual Sapien + cloth TAVI device, tested for valve-in-valve application exhibited ≈ –3.3 mL/s leakage rate with 100 mmHg transvalvular pressure (34). While the PDVA error was apparent due to translucency of the closed mTAVI device, it was negated by insertion of PDVA =0, as justified by the minimum static leakage rates. Due to signal bandwidth differences, minor temporal adjustment between the PDVA and the other signals mitigated phasing error (35). Leakage occurs in residual hidden intra and paravalvular areas, where passage of backlight is obstructed, limits direct characterization of such regions by the PDVA.

### Derivations and data compensations

**Transvalvular flows attributable to compliance:** transvalvular flow signals were measured by an electromagnetic flow probe with mid-plane ≈4.2 cm proximal to the test valve mid-plane. The closed valve state occurs at minimum PDVA. Transitional
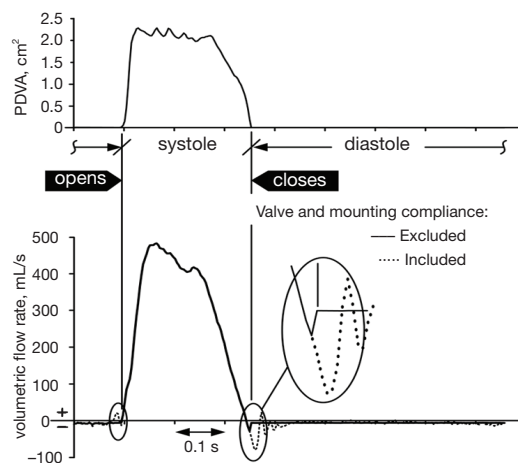


**Figure S1** Valve motion waveform (PDVA) for mock-TAVI (mTAVI) device identifies initial moments when the device "opens" and "closes" (vertical timing lines). Volumetric flow rate waveform (lower-panel) shows compliance related confounding flows (dotted-line) and post experiment mitigation (solid-line). Replacement of the compliance "Included" data with compliance "Excluded" data is performed post experiment.

flow signals include both compliance related flows and those that actually traverse flow pathways. Importantly, our methodology distinguishes between flows caused by compliant structures that have no net energy loss shown in *Figure S1*; (dotted-line) from those that actually incur energy loss (solid-line). Left uncorrected, hybrid flow signals (dotted-line) near valve opening and closing results in underestimation of the disparity in regurgitant flow between mechanical and tissue type heart valves. Recognition and correction of compliance mediated flow (dotted-line) as exemplified by the solid line, must be taken into consideration for other *in vitro* and *in vivo* methodologies that quantify valve performance including: transthoracic (TTE) and transesophageal (TEE) echocardiography, Magnetic Resonance Imaging (MRI), Laser Doppler Anemometry (LDA), Particle Imaging Velocimetry (PIV) and Computational Fluid Dynamics (CFD). By recognizing the closed valve interval when PDVA is minimal, our methodology reassigns with closed valve data determined from a separate leakage test described subsequently. Compliance correction benefit is qualitatively exemplified in *Figure S1*, where approximate reductions are realized for: valve closing volumes (82%), peak volumetric backflow rates (76%), and closure times (18 ms).

In *Figure S2*, hydrodynamic and valve motion (PDVA) waveforms for a St Jude Medical (SJM), an Edwards-
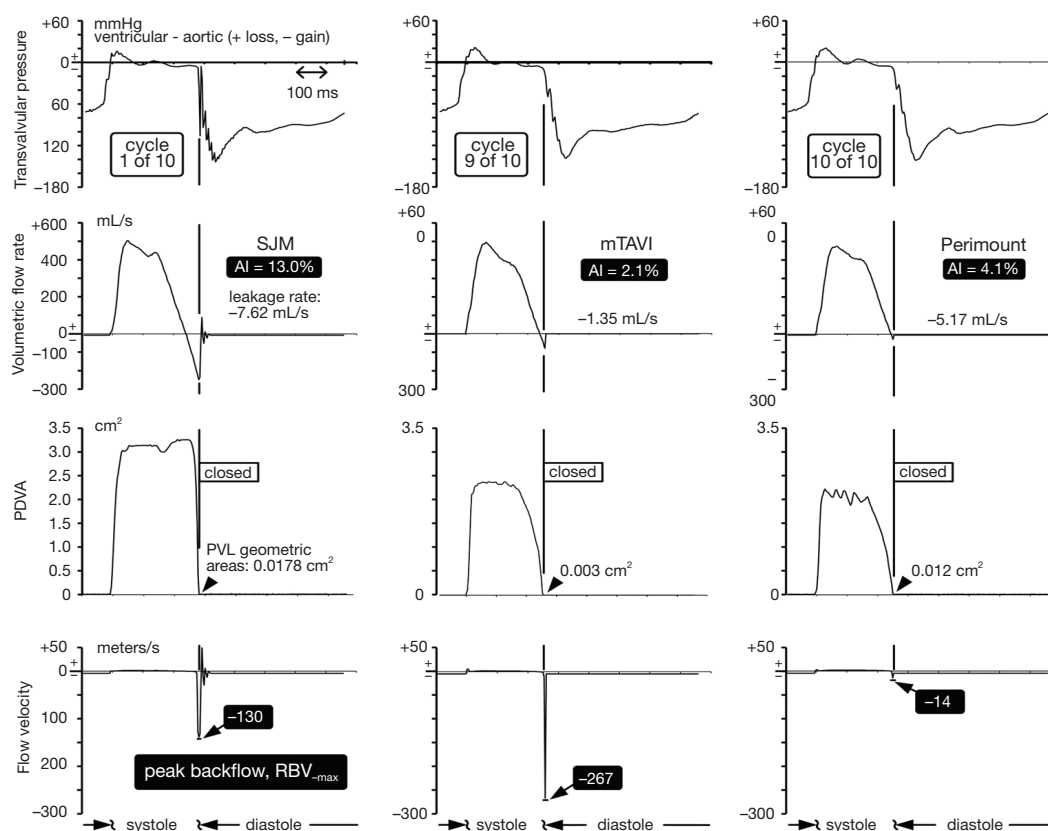
**Figure S2** Additional waveforms of hydrodynamic and valve motion (PDVA) waveforms for a St Jude Medical (SJM), an Edwards-Perimount pericardial valve, and the mock-TAVI (mTAVI) device for comparative regional backflow velocity (RBV) perspective. See *Figure 2A* caption for other test conditions.

Perimount pericardial valve, and the mock-TAVI (mTAVI) device for comparative regional backflow velocity (RBV) perspective. For the mTAVI device, a leakage rate substantially lower than for the SJM is associated with an $RBV_{-max}$ of −267 meters per second (m/s) and a thrombogenic potential perhaps equivalent to or exceeding that of mechanical heart valves (MHV). See *Figure 2A* caption for other test descriptors.

**Geometric leakage area versus leakage rate by means of calibration orifices:** previously, measurement of total residual leakage area entailed backlighting closed valve areas assuming light would pass directly through the residual areas with negligible reflection in those regions and separately estimating leakage areas in regions hidden from backlight illumination (35). Presently, we utilize a leakage tester (*Figure S3*), to measure volumetric leakage flow rate under simulated conditions typical of trans-aortic closed valve mean

pressure (≈100 mmHg). Leakage rate (mL/s) was determined by dividing the measured volume of test fluid between the sensors (≈91 mL) by the timer reading(s). For calibration, an orifice shown in the top panel of *Figure S4* was machined from aluminum to emulate very small leakage areas with 36 small holes, each of length ≈0.55 mm and 0.457 mm diameter consisted of six sets of holes and 6 holes per set. The hole centers and sets were equally spaced at 6.2° and 60°, respectively. Although leakage rate has a binary dependence on viscosity and total leakage area, flow in different gap shapes with the same fluid viscosities and geometric areas will present different boundary layers and extensions. With the calibration orifice utilized here, there is no fixed percentage difference in leakage rate versus fluid viscosity. For example, with a leakage area of 0.010 cm$^2$, the approximate difference is 9.7% whereas with 0.060 cm$^2$, the difference is 13.2%.

Prototype specifications for enhanced Leonardo$^{VSI}$ test system used in this study:

Page 10 of 10

Scotten and Siegel. Thrombogenic potential of TAVI with trivial PVL
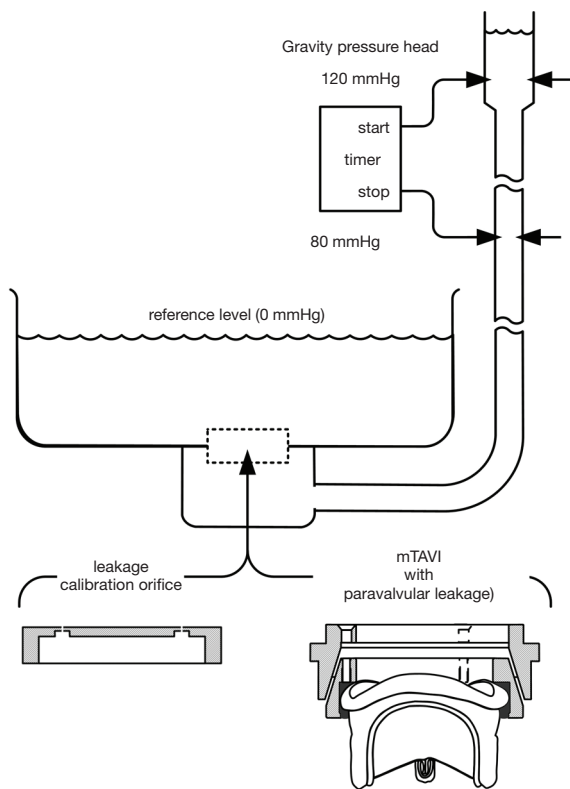
**Figure S3** Apparatus for calibration of the leakage orifice (geometric leakage area versus volumetric leakage rate) and for measuring closed mock-TAVI (mTAVI) device volumetric leakage rate preset for various paravalvular leakages (PVL). Knowing mTAVI device leakage rate, total residual backflow area can be determined by means of the leakage orifice calibration. The mTAVI device is evaluated for leakage prior to pulsatile flow testing.

- Temporal resolution ≈1.04 µs;
- Spatial area resolution (closed valve), 0.001 cm$^2$ (n=10 cycle average);
- Telecentric lens maintains constant magnification ≈0.16×;
- Working distance ≈18 cm;
- Perspective error <0.3% (depth 15 mm);
- Spatial sensitivity variation <6%;
- LED back light (red):
  - Wavelength 625 nm, ±15 nm;
  - Uniformity 99.24%;
  - Luminance 5,780 cd/m$^2$;
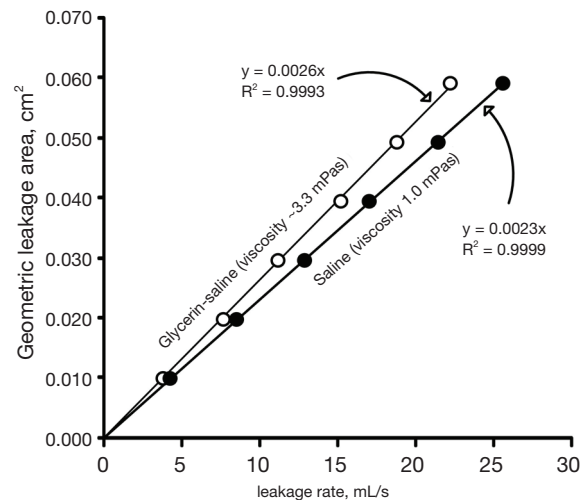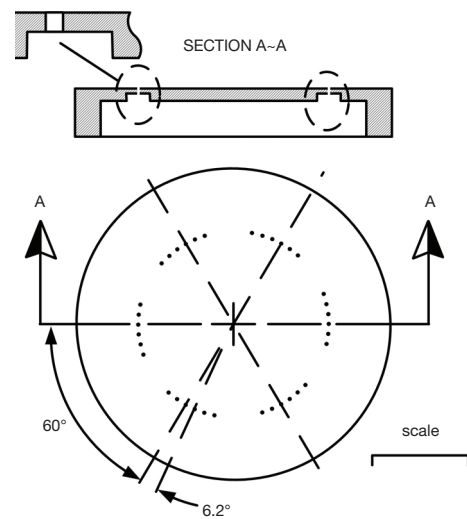  - Typical linear calibration: y=0.00128x, with R$^2$=0.9998.



**Figure S4** Diagram of leakage orifice (top panel) and calibrations for fluids with different viscosity (saline and glycerin-saline). The six sets of holes were sequentially blocked thus obtaining six data pairs for each calibration line. For very small leakage pathways, the primary determinant of leak flow rate is the total geometric leakage flow area.

## References

34. Walther T, Dehdashtian MM, Khanna R, et al. Transcatheter valve-in-valve implantation: in vitro hydrodynamic performance of the SAPIEN+cloth trans-catheter heart valve in the Carpentier-Edwards Perimount valves. Eur J Cardiothorac Surg 2011;40:1120-6.
35. Scotten LN, Siegel R. Importance of shear in prosthetic valve closure dynamics. J Heart Valve Dis 2011;20:664-72.